

# Analysis and Implementation of Real Number Extended Sliding Surface with Integral Compensation for DC-AC Converters

E C Chang<sup>1</sup>, R C Wu and K Y Liao

Department of Electrical Engineering, I-Shou University, Kaohsiung City 84001, Taiwan, R.O.C.

E-mail: enchihschang@isu.edu.tw

**Abstract.** This paper proposes a real number extended sliding surface (RNESS) with integral compensation (IC) for the application of DC-AC converters. Classic sliding surface (CSS) is insensitive to system uncertainties, but in sliding action its system dynamics becomes a reduced-order dimension and thus lost the partial system dynamics. For recovering incomplete system response, the RNESS is designed and can retrieve incomplete system response of the CSS. However, steady-state errors still exist in system dynamics of the RNESS and cause high converter voltage harmonics. To overcome steady-state errors, a modified RNESS by the addition of IC is proposed. With the proposed method, the system yields a DC-AC converter with high-quality AC output voltage. Experiments are performed in support of the proposed method.

## 1. Introduction

DC-AC converters have been extensively used in many AC power conditioning systems. The DC-AC converters need to be demanded high-quality AC output voltage of low THD and fast dynamic response, and these can be obtained by employing feedback control. The control of the DC-AC converters is popularly designed through sliding surface control; however, the CSS is adopted, and thus incurs incomplete dynamics response [1-3]. To recover lost system dynamics, the RNESS is applied to DC-AC converters. However, steady-state errors still exist in DC-AC converters, and cause serious voltage harmonics [4], [5]. Thus, by combining a RNESS with IC (RNESS-IC), steady-state errors can be overcome and a closed-loop DC-AC converter will yield good performance under various loading. The proposed method is implemented digitally using a CPLD development board. Experiments are given to verify the effectiveness of the proposed method.

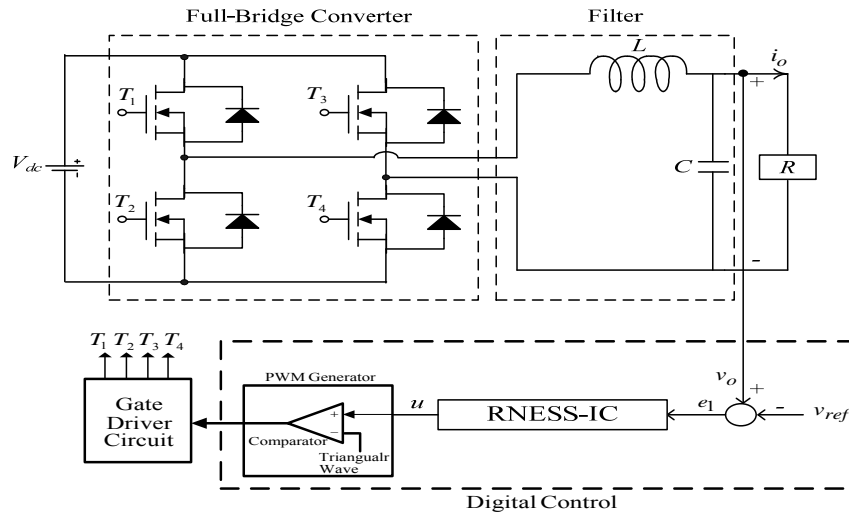
## 2. Mathematical Modeling of DC-AC Converter

Figure 1 shows the block diagram of a DC-AC converter, and the system dynamics can be written in the following.

---

<sup>1</sup> Corresponding Author: E C Chang is with the Department of Electrical Engineering, I-Shou University, No.1, Sec. 1, Syuecheng Rd., Dashu District, Kaohsiung City 84001, Taiwan, R.O.C. This work was supported by the Ministry of Science and Technology of Taiwan, R.O.C., under contract number MOST103-2221-E-214-027.





**Figure 1.** Block diagram of DC-AC converter.

$$\begin{bmatrix} \dot{e}_1 \\ \dot{e}_2 \end{bmatrix} = \underbrace{\begin{bmatrix} 0 & 1 \\ -\frac{1}{LC} & -\frac{1}{RC} \end{bmatrix}}_{\text{system matrix}} \begin{bmatrix} e_1 \\ e_2 \end{bmatrix} + \underbrace{\begin{bmatrix} 0 \\ 1 \end{bmatrix}}_{\text{control matrix}} u + \underbrace{\begin{bmatrix} 0 \\ -\frac{1}{LC} v_{ref} - \frac{1}{RC} \dot{v}_{ref} - \ddot{v}_{ref} \end{bmatrix}}_{\text{external interference}} \quad (1)$$

Thus, once the control signal  $u$  is designed well, the converter's output will remain the same as what is desired  $v_{ref}$ .

### 3. RNESS-IC Control Design

Generally, a CSS is constructed as

$$\sigma = \ker(C) \subset \mathfrak{R} \quad (2)$$

where  $C \in \mathfrak{R}^{m \times n}$ , and  $\text{rank}(C) = m$ .

The resulting closed-loop dynamics yields

$$\begin{bmatrix} \dot{x} \\ \dot{y} \end{bmatrix} = \begin{bmatrix} R_e A_e & 0 \\ 0 & R_e A_e \end{bmatrix} \begin{bmatrix} x \\ y \end{bmatrix} + \begin{bmatrix} 0 \\ B \end{bmatrix} u; \quad A_e = \text{system matrix} \quad (3)$$

From (2) and (3), the system dynamics is  $(n-m)$  reduced-order dimension, and deteriorates system performance. To recover the incomplete system dynamics, the RNESS will be designed as follows.

Firstly, defining the  $u$  and  $x$  with the pairs of complex conjugate  $(v, \bar{v}$  and  $z, \bar{z})$  as

$$u = \frac{1}{2}(v + \bar{v}) \quad (4)$$

$$x = \frac{1}{2}(z + \bar{z}) \quad (5)$$

where  $v, \bar{v} \in C^m$  and  $z, \bar{z} \in C^n$ .

Substituting (4) and (5) into (3), the real system (3) yields the sum of the two complex system

$$\dot{z} = Az + Bv \quad (6)$$

$$\dot{\bar{z}} = A\bar{z} + B\bar{v} \quad (7)$$

Then, a real number extended sliding surface is designed as

$$\gamma = \Psi z = 0 \quad (8)$$

$$z = \begin{bmatrix} x_1 & \dots & x_m & \dot{x}_1 & \dots & \dot{x}_m \end{bmatrix}^T \quad (9)$$

where  $\Psi \in C^{m \times n}$ .

The sliding function matrix can be partitioned compatibly as

$$\Psi = \begin{bmatrix} \Psi_1 & \Psi_2 \end{bmatrix} = \begin{pmatrix} M_{11} + iN_{11} & & & 1 & & \\ & \ddots & & & \ddots & \\ & & & & & \\ & & & M_{mm} + iN_{mm} & & \\ & & & & & 1 \end{pmatrix} \tag{10}$$

where  $\Psi_1 \in C^{m \times (n-m)}$  and  $\Psi_2 \in C^{m \times m}$ .

The system matrix thus becomes

$$A_z = (I - B(\Psi B)^{-1} \Psi)A = \begin{bmatrix} A_{11} - A_{12} \Psi_2^{-1} \Psi_1 & A_{12} \\ 0 & 0 \end{bmatrix} \tag{11}$$

Letting  $z = x + iy$ , we obtain

$$\begin{aligned} \bar{z} + \dot{z} &= A_z(x + iy) + \bar{A}_z(x - iy) \\ &= 2(\text{Re } A_z x - \text{Im } A_z y) \end{aligned} \tag{12}$$

Contrariwise,

$$\begin{aligned} \bar{z} - \dot{z} &= A_z(x + iy) + \bar{A}_z(x - iy) \\ &= 2(\text{Im } A_z x + \text{Re } A_z y) \end{aligned} \tag{13}$$

Therefore, the  $\mathfrak{R}^{2n}$  dimensional system exists

$$\begin{bmatrix} \dot{x} \\ \dot{y} \end{bmatrix} = \begin{bmatrix} \text{Re } A_z & -\text{Im } A_z \\ \text{Im } A_z & \text{Re } A_z \end{bmatrix} \begin{bmatrix} x \\ y \end{bmatrix} \tag{14}$$

The classic situation can be verified as  $\Psi = \sigma$ , here  $\Psi$  is a real linear map, then the (14) has

$$\begin{aligned} \begin{bmatrix} \dot{x} \\ \dot{y} \end{bmatrix} &= \begin{bmatrix} \text{Re } A_z & 0 \\ 0 & \text{Re } A_z \end{bmatrix} \begin{bmatrix} x \\ y \end{bmatrix} \\ &= \begin{bmatrix} (I - B(CB^{-1}C)A) & 0 \\ 0 & (I - B(CB^{-1}C)A) \end{bmatrix} \begin{bmatrix} x \\ y \end{bmatrix} \end{aligned} \tag{15}$$

The control signal is assumed as the following form

$$\begin{aligned} v &= -\underbrace{(\Psi B)^{-1} \Psi A_z}_{u_{ez}} \\ &\quad - \underbrace{(\Psi B)^{-1} \Psi A_z [F \text{sign}(\text{Re } \gamma) + iG \text{sign}(\text{Im } \gamma)]}_{u_{sz}} \end{aligned} \tag{16}$$

where  $u_{ez}$  is the equivalent control and  $u_{sz}$  represents a discontinuous switching control component.

Define  $v = u + iw$ , (4) and (16) lead to

$$\begin{aligned} u &= -\text{Re } (\Psi B)^{-1} \Psi A x + \text{Im } (\Psi B)^{-1} \Psi A y \\ &\quad - \text{Re } (\Psi B)^{-1} F \text{sign}(\text{Re } \gamma) + \text{Im } (\Psi B)^{-1} G \text{sign}(\text{Im } \gamma) \end{aligned} \tag{17}$$

and

$$\begin{aligned} w &= -\text{Im } (\Psi B)^{-1} \Psi A x + \text{Re } (\Psi B)^{-1} \Psi A y \\ &\quad - \text{Im } (\Psi B)^{-1} F \text{sign}(\text{Re } \gamma) - \text{Re } (\Psi B)^{-1} G \text{sign}(\text{Im } \gamma) \end{aligned} \tag{18}$$

Suppose  $\Psi = M + iN$ , the (17) and (18) is rewritten as

$$\begin{aligned} \begin{bmatrix} u \\ w \end{bmatrix} &= -\begin{bmatrix} \text{Re } (\Psi B)^{-1} \Psi A & \text{Im } (\Psi B)^{-1} \Psi A \\ \text{Im } (\Psi B)^{-1} \Psi A & \text{Re } (\Psi B)^{-1} \Psi A \end{bmatrix} \begin{bmatrix} x \\ y \end{bmatrix} \\ &\quad + \begin{bmatrix} \text{Re } (\Psi B)^{-1} F & \text{Im } (\Psi B)^{-1} G \\ \text{Im } (\Psi B)^{-1} F & \text{Re } (\Psi B)^{-1} G \end{bmatrix} \\ &\quad \cdot \text{sign} \left( \begin{bmatrix} M & -N \\ N & M \end{bmatrix} \begin{bmatrix} x \\ y \end{bmatrix} \right) \end{aligned} \tag{19}$$

Employing  $y = 1/2(z - \bar{z})$ , the differential equation can be obtained as

$$\dot{y} = Ay + Bw \tag{20}$$

Thus, the resulting system is shown in (21) into  $\mathfrak{R}^{2n}$  dimension, and thus recovers all the dynamics lost in the CSS design process as follows:

$$\begin{bmatrix} \dot{x} \\ \dot{y} \end{bmatrix} = \begin{bmatrix} R_e A_z & -I_m A_z \\ I_m A_z & R_e A_z \end{bmatrix} \begin{bmatrix} x \\ y \end{bmatrix} + \begin{bmatrix} B & 0 \\ 0 & B \end{bmatrix} \begin{bmatrix} u_{swz} \\ w_{swz} \end{bmatrix}, \quad \begin{matrix} u_{ez} = \text{equivalent control} \\ w_{sz} = \text{sliding control} \end{matrix} \tag{21}$$

Notice that the (1) with external interferences cause steady-state errors, and thus an IC  $u_{ic} = \int e_1 dt$  is introduced to overcome steady-state errors. Finally, the proposed control law is  $u = u_{ic} + u_{ez} + iw_{sz}$ .

#### 4. Experimental Results

The proposed system parameters are as follows:  $V_{dc}=200$  V;  $v_o=110$  V<sub>rms</sub>,  $f=60$  Hz;  $L=1$  mH;  $C=30$   $\mu$ F; Switching Frequency  $f_s=12$  kHz;  $R_{rated}=10$   $\Omega$ . For no load to full load, the results with the RNESS-IC and CSS are shown in Figure 2 and Figure 3, respectively. The output voltage with the RNESS-IC only dips lightly, but the large voltage dip occurs in the CSS. For rectifier load ( $C_d = 200$   $\mu$ F  $\cdot R_d = 45$   $\Omega$ ) shown in Figure 4, the output voltage with the RNESS-IC is close to sinusoidal waveform (%THD=2.01%), but that with the CSS shown in Figure 5 has a high %THD of 6.23%.

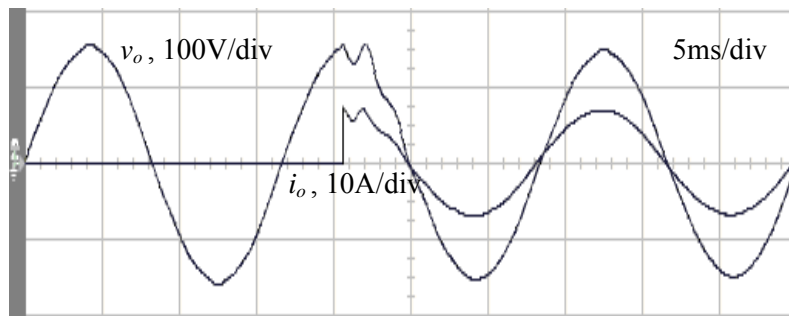


**Figure 2.** Converter output waveform from no load to full load with RNESS-IC.

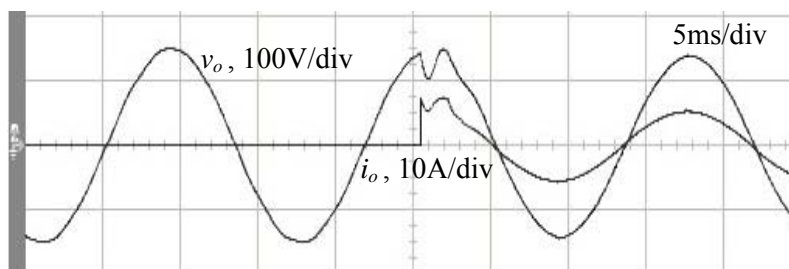


**Figure 3.** Converter output waveform from no load to full load with CSS.

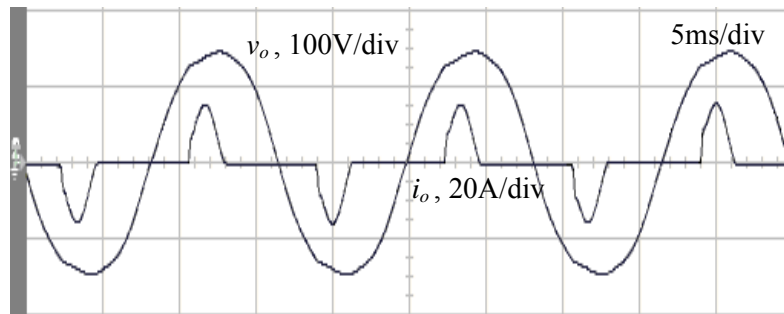


**Figure 4.** Converter output waveform under rectifier load with RNESS-IC.

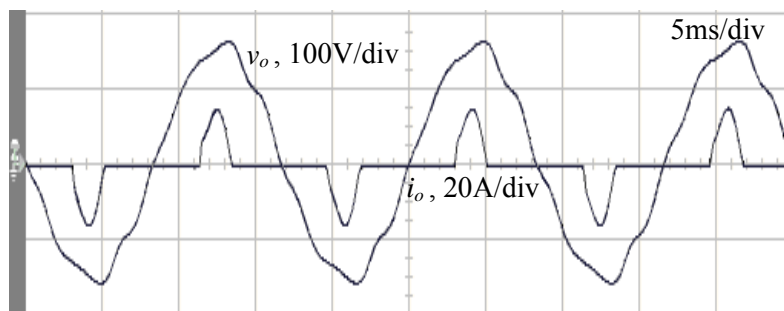


**Figure 5.** Converter output waveform under rectifier load with CSS.

## 5. Conclusions

The proposed converter recovers lost system dynamics and overcomes steady-state errors. Experiments show that the proposed system surpasses the results achieved under the classic system. Therefore, it is clear that the proposed method is robust in transient loading and steady-state loading.

## 6. Acknowledgment

This work was supported by the Ministry of Science and Technology of Taiwan, R.O.C., under contract number MOST103-2221-E-214-027.

## 7. References

- [1] Tan S C, Lai Y M and Tse C K 2012 *Sliding Mode Control of Switching Power Converters: Techniques and Implementation* (Boca Raton: CRC Press)
- [2] Abrishamifar A, Ahmad A and Mohamadian M 2012 Fixed switching frequency sliding mode control for single-phase unipolar inverters *IEEE Trans. Power Electronics*, vol 27, no 5, pp 2507-2514
- [3] Yang X., Liu T, Huang L and Chen W J 2013 A sliding-mode controller with multiresonant sliding surface for single-phase grid-connected VSI with an LCL filter *IEEE Trans. Power Electronics*, vol 28, no 5, pp 2259-2268
- [4] Shepit B M and Pieper J K 2001 Sliding mode control design for complex valued sliding manifold *Proc. Conf. IEEE Decision and Control* vol 1 pp 920-921
- [5] Shepit B M, and Pieper J K 2003 Sliding-mode control design for a complex valued sliding manifold *IEEE Trans. Automatic Control* vol 48 no 1 pp 122-127